Self Welding Behavior of Various Materials in Sodium Environments (II) Self-Welding of Hard Metals and Carbide Materials

Jan., 1975

POWER REACTOR AND NUCLEAR FUEL DEVELOPMENT CORPORATION

〒319-1184　茨城県那珂郡東海村大字村松4番地49
核燃料サイクル開発機構
技術展開部　技術協力課

Inquiries about copyright and reproduction should be addressed to:
Technical Cooperation Section,
Technology Management Division,
Japan Nuclear Cycle Development Institute
4-49 Muramatsu, Tokai-mura, Naka-gun, Ibaraki, 319-1184
Japan

T N951 74-12
Jan., 1975

Self-Welding Behavior of Various Materials in Sodium Environments (II)

Self-Welding of Hard Metals and Carbide Materials

S. Mizobuchi*,
S. Kano*,
M. Namekawa*,
T. Owada*, and
H. Atsumo*

Abstract

This experiment was conducted from October 1 to December 21, 1973 for the purpose of comparing the self-welding behavior of various kinds of material in high temperature sodium, thus acquiring the basic knowledge of their self-welding phenomena.

In our previous report (SN941 73-32), we have taken up the subject self-welding between hard Cr plating and SUS 316 (equivalent to AISI Type 316 Stainless Steel). This time, however, we have undertaken the tests of carbide materials, refractory materials such as molybdenum and tungsten well as stellite No. 6, nickel, nichrome, etc. The tests have revealed the following results:

1. Chrome-carbide (Detonation Gun-coated) has a good self-weld resistance. But, the carbide with the content of tungsten showed a strong tendency the self-welding.
2. Tungsten and molybdenum had strongly resistance against self-

---

This is the translation of the report, No. N941 74-18, issued in March, 1974.

* Sodium Engineering Division, Oarai Engineerint Center, PNC.

welding effective as material.

3. Stellite No. 6 combined with SUS316 showed a tendency to self-welding.
4. Nickel and nichrome showed complete self-welding by forming a diffusion layer in the boundary zone.

Thus, it has been confirmed by this experiment that such self-welding phenomena appearing in those components contacting with each other in high temperature sodium are the problems not to be regarded lightly since any mistake in selecting materials for these components might lead to serious problems. It is, therefore, desired that more efforts be devoted to the development of self-weld resistant materials suitable to each components by a long-term experiment in the future.

CONTENTS

1. Preface

Components or parts which contact with each other or make sliding motion in sodium are subject to such phenomena as self-welding, friction and wear, which are the potential factors for various kinds of operational troubles. In a fast breeder reactor, potential trouble spots include the fuel assembly duct pad, the driving part of control rods, pads on the inside and outside of the guide tube, guide roller pins and dash-pot, grippers, entrance nozzle and its receptacle, parts of the clamping mechanism, in-vessel-handling-machine, etc. These are all different in their environment, temperature, configuration, contacting pressure, sliding mode, etc., and also the materials of their partner parts or components are quite different. Therefore, it is important to select adequately partner materials.

Since 1972, we have been carrying out a series of self-welding and wear tests, and in our previous report,[1] we have presented findings on self-welding behaviors on mainly SUS 316 stainless steel and hard chrome plating. This time, experiments have been undertaken relating to two refractory metals (W and Mo), and carbide materials. Especially, it has been said hitherto that it is effective[2] to give self-weld resistant property by lining such ductile mother materials as SUS 316 with these materials. In this respect, it was tried last time with the use of partial plasma coated layer. But this time, self-welding tests by means of a detonation gun (hereinafter called D-Gun) and a wire-explosion (hereinafter called W-E process), which was developed in Japan and effective for lining of interior of small holes, were respectively undertaken on various materials in high temperature sodium.

2. Test Method

2-1. Test and Test Conditions

The previously employed test apparatus was used for the present test, which employed F-2 pot of the Low Purity Material Test Loop. The test conditions are as shown in the following Table 1:

Table 1. Test Conditions

Specimen No.	Na Temp. (℃)	Dwell time (hr)	Test load (Kg)	Na flow rate (ℓ/min)
1 ~ 1 ~ 1 ~ 17	600	200	627	0.3
2 ~ 1 ~ 2 ~ 17	600	200	600	0.3

2-2. Configuration and Chemical Composition of Test Pieces and Their Manufacturing Method

The dimensions of test piece are shown in Fig. 1. Both the upper and lower faces of the test piece are for the test contact faces in the present test, and the surface contacting area are 220 mm^2 and 8.4 mm^2 respectively. The chemical composition of the materials tested are given in the following Table 2:

Table 2. Chemical Composition of Materials (Wt %)

Materials	C	Si,	Ni,	Cr,	Fe,	Mn,	B,	Mo,	W,	Co,
Stellite No6	1.04	1.17		28.65	0.27				4.20	Bal
SUS 316	0.07	0.48	10.5	16.61	Bal	1.53		2.12		
Mo								Bal		
W									Bal	
Ni			Bal							
Ni-Cr			Bal	20						
Hard chrome plating				Bal						
G - 2	94 % WC + 6 % Co									
LC-IC	85 % Cr_3C_2 + 15 % Ni -Cr									
LW - 5	25 % WC + 5 % Ni + W - Cr Carbide									

The manufacturing method of each test pieces is shown in the following Table 3:

Table 3. Manufacturing Method of Specimens

Materiarls	Manufacturing Methods
IC-IC LW-5	Detonation Gun Coating on 316SS, Lapped
IC-IC Mo W	Plasma Gun Coating on 316SS, Lapped
Mo W Ni Ni-Cr G-2	Wire Explosion Coating on 316SS, AS Sprayed, or Lapped,
Hard Crome	Electroplationg on 316SS, AS Plated, or Lapped,
Stellite №6	Oxy-Acetylene Gas Weld, Lapped,

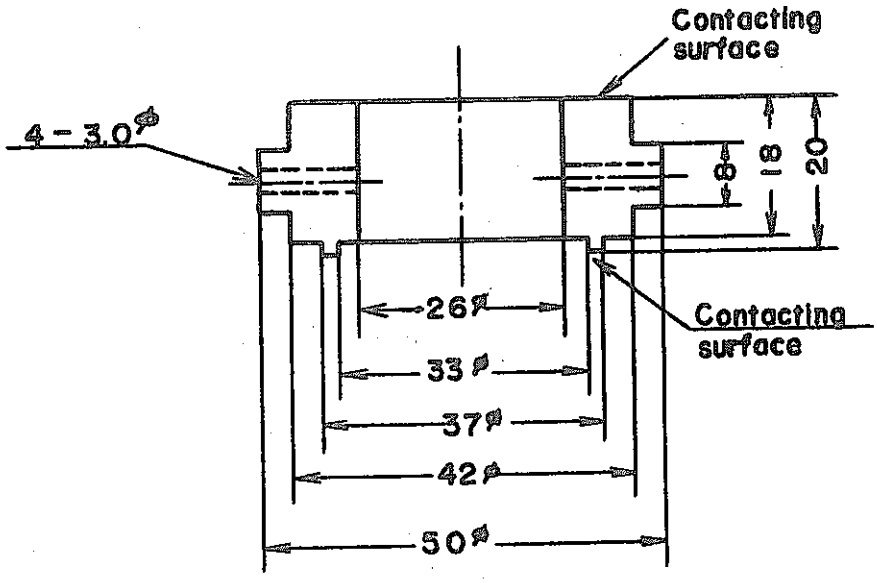

Fig. 1. Dimensions of Specimen

The sketch drawing of D-Gun is shown in the following Fig. 2.

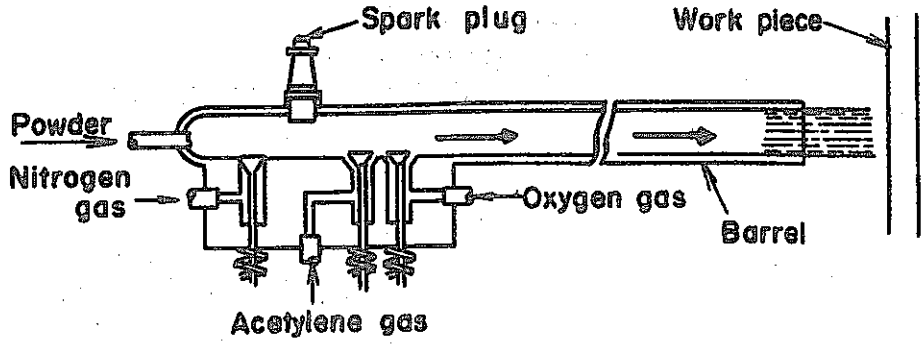

Fig. 2. Sketch of Detonation Gun

The principle of padding in the manufacture of these test pieces is briefly given as follows:

In the first place, put some powder into a tube, then fill it with oxygen and acetylene, and ignite it with a spark plug to make it explode so that the powder will fuse and sprayed to the mother material at high speed. This gives the coating a strong adhesion strength.

Fig. 3 shows a sketch drawing of a plasma gun:

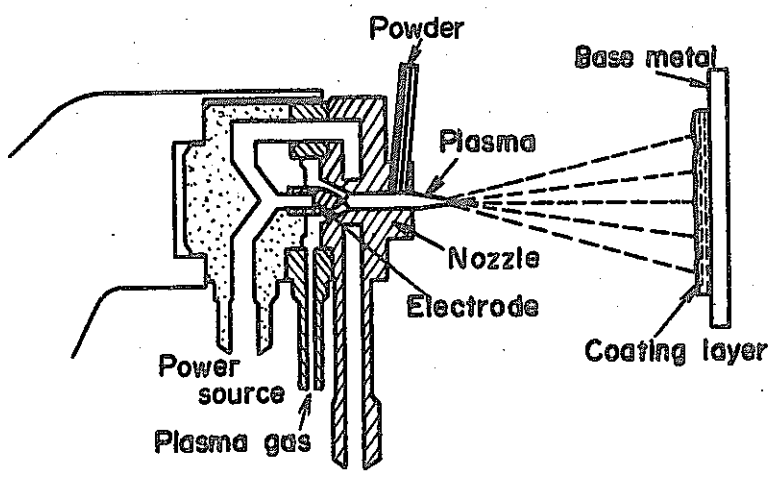

Fig. 3. Sketch of Plasma Gun

This spraying method by means of plasma jet has been in use conventionally. Its features are that as the temperature of the plasma jet is 10,000 °K - 20,000 °K, the powder passing through the gun is heated, fused and sprayed to the mother material. The spray speed is slower than in the case of the above mentioned detonation gun. The following W-E method has been developed in Japan, and is considered as the one of the most prospective methods. Its principle is shown in Fig. 4.

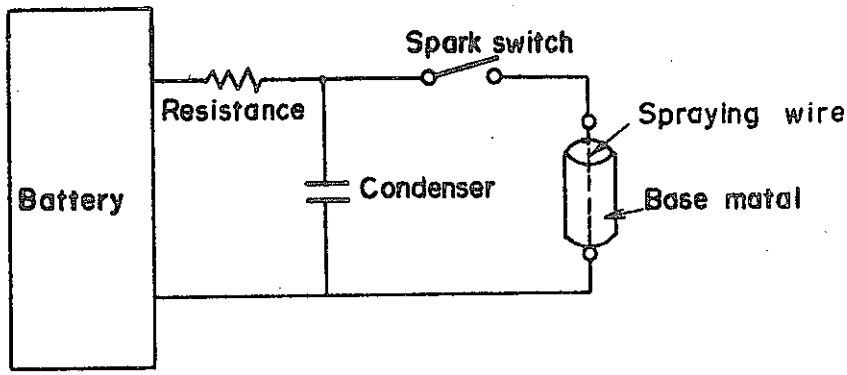

Fig. 4. Fundamental Sketch of Spark Discharge

This spark discharge method is to coat the base material with a layer of the exploded powder by spark-exploding the discharge material by passing impulse high-power current. The features of this method are in the fact that, unlike other spark discharging methods, it has made it possible to spray inside any tubular material, thus having overcome the greatest weakpoint of this spray method. A disadvantage of this method is that only such material that has electrical conductivity can be fusion sprayed. It is however advantageous in all respects that such coating material can be cold sprayed to give the wear resistance and self-weld resistance on contacting surface. Therefore, it is expected that this technology

trouble of "galling" and "self-welding" on each component when properly applied to the inside structures of a fast breeder reactor to provide them with self-weld resistant and wear resistant properties.

2-3. Method of Analysis

The test pieces which have been subjected to in-sodium test are taken out from the pot, and are treated by ethyl-alcohol, and then go through the processes of washing, supersonic wave washing by acetone, and drying, and then are maintained in a desiccator until the actual analysis. The analysis is performed according to the previously reported procedures[1] of which items are given in Fig. 5. The self-welded specimens were cut apart and were subjected to microscopic observation of their cohesion boundary regions and the ultimate analysis by XMA. Also, for the measurement of cohesion strength, tensile fracture tests were performed by an INSTRON tester. The fractured test pieces were measured of the roughness on the fractured surfaces. This is one of the

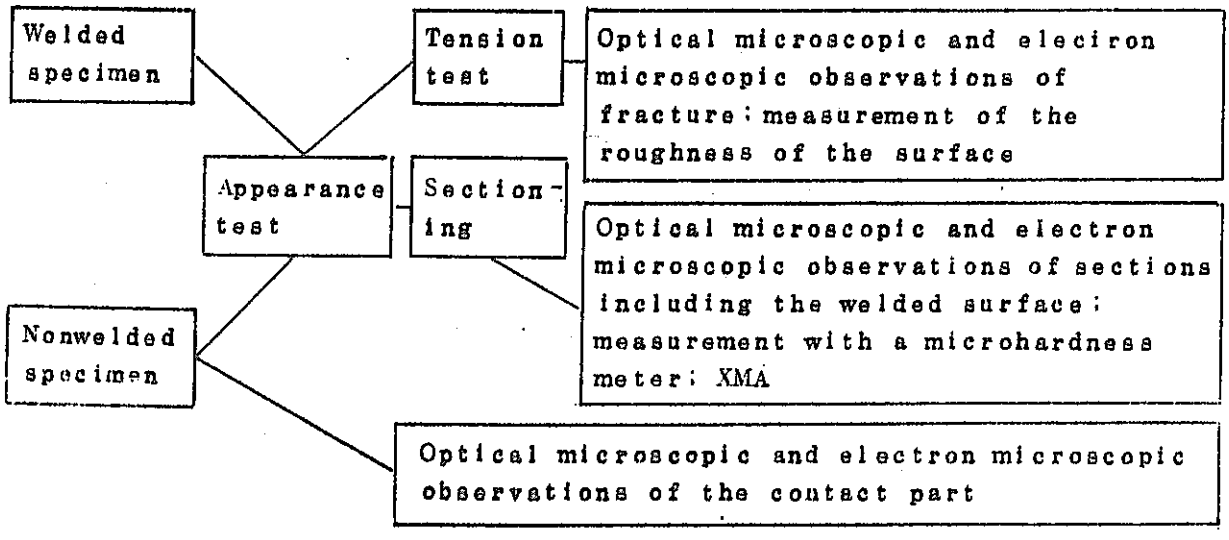

Fig. 5. Analytical procedure

important items to determine the change of surface roughness by material transfer in the area where cohesion has taken place and to know its effect on the friction coefficient thereafter.

3. Test Results and Discussion

Weldability was found to be considerably strong for the test pieces which remained in contact even after ultrasonic washing. But even in the case of such combination of materials, their actual cohesion phenomenon might have been originated by the presence of sodium impregnated into their interface region due to their surface roughness. For this reason, a further study may be necessary by the tensile test and by means of microscopic observation on the fractured surface after tensile rupture test. Table 4 summarises the results of the test of the combination of test-pieces:

Table 4. Summary of the results of self-welding tests

Specimen No.	Combination of materials			Weldability
1 - 1	SUS 316	VS.	SUS 316	○
1 - 2	Cr plating①	VS.	Cr plating①	×
1 - 3	Cr plating①	VS.	SUS 316	×
1 - 4	G — 2②	VS.	SUS 316	×
1 - 5	G — 2②	VS.	Mo②	×
1 - 6	Mo②	VS.	SUS 316	×
1 - 7	Mo③(lapped)	VS.	SUS 316	○
1 - 8	Ni-Cr②	VS.	SUS 316	○
1 - 9	Ni-Cr②	VS.	Ni②	○
1-10	Ni②	VS.	SUS 316	○
1-11	SUS 316	VS.	SUS 316	○
1-12	SUS 316	VS.	LCIC④	○
1-13	SUS 316	VS.	SUS 316	○
1-14	LW 5④	VS.	SUS 316	○
1-15	SUS 316	VS.	W②	×
1-16	W②	VS.	stellite No6⑤	×
1-17	stellite No6⑤	VS.	SUS 316	×
2- 1	SUS 316	VS.	Ni②	○
2 - 2	Ni②	VS.	SUS 316	○
2- 3	SUS 316	VS.	Ni-Cr②	○
2 - 4	Ni-Cr②	VS.	SUS 316	○
2 - 5	SUS 316	VS.	G — 2②	×

Specimen No.	Combination of materials			Weldability
2 - 6	G – 2②	VS.	Mo②	○
2 - 7	Mo②	VS.	SUS 316	×
2 - 8	SUS 316	VS.	Mo③	×
2 - 9	SUS 316	VS.	W②	○
2 -10	W②	VS.	SUS 316	○
2 -11	W③	VS.	LCIC④	×
2 -12	SUS 316	VS.	SUS 316	○
2 -13	LCIC④	VS.	LCIC①	×
2 -14	SUS 316	VS.	LW5①	○
2 -15	SUS 316	VS.	stellite No6⑤	○
2 -16	stellite No6⑤	VS.	SUS 316	×
2 -17	SUS 316	VS.	SUS 316	○

Here, the symbol ○ in the "weldability" column represents those material combinations which remained adhered even after the ultrasonic wave cleaning, while the symbol × represents those which have been apart from each other.

Table 5 represents the results of the tensile fracture test of the self-welded test-pieces.

F column represents the load values (kg) required for fracture under room temperature of the test pieces which suffered cohesion. K value is expressed by $K = \frac{F}{P}$. Here P is the load applied to the test piece during the test. The reason for two different contact pressures of 2.7 kg/mm^2 and 0.7 kg/mm^2 is that the area on the

Table 5. Results of the tensile test of Self-welded specimens

Specimen No.	Combination of materials	Contact pressure (Kg/mm²)	F (Kg)	K
2- 2	SUS 316 VS. Ni	2.7	658	1.1
2- 3	SUS 316 VS. Ni-Cr	2.7	672	1.12
2- 6	G — 2 VS. Mo	2.7	20	0.03
2- 9	SUS 316 VS. W	2.7	91	0.15
2-14	SUS 316 VS. LW5	2.7	270	0.45
2-15	SUS 316 VS. stellite No6	2.7	245	0.4
2- 4	SUS 316 VS. Ni-Cr	0.7	442	0.74
2-10	SUS 316 VS. W	0.7	30	0.05
2-12	SUS 316 VS. SUS 316	0.7	193	0.32

upper face and that of the lower face of the test piece are different. Because of this, in the case of materials of easy cohesion such as Ni, and Ni-Cr, even if taking a large contacting area and the smaller apparent contacting pressure, the total cohesion strength does not decline very much. That is, it appears the effect of the true area of the contact surface is larger than that of the apparent contacting pressure. Table 6 represents the measurement of the average surface roughness of the test pieces both before and after tests (after tensile fracture for the test pieces with self-welding). As indicated by Table 6, SUS 316 coupled with Ni, Ni-Cr and LW-5 indicate an extremely large surface roughness on the part of SUS 316. This is thought as the result of a complete transfer of the partner material to SUS 316 after tensile fracture. In this case, because of the roughness on the surface, subsequent deterioration of friction characteristics can be expected. SUS 316 combined with the same partner has a strong cohesion tendency, but their surface roughness change is minimal. Although indicated a small roughness change from 0.2 μ

Table 6. Surface Roughness of the Specimens before and after Testing

Specimen No	(Measured) Materials	(Opposed) Materials	Roughness Change (μ) before	Roughness Change (μ) after	Remarks
2-2	SUS 316	(Ni)	0.2	14	
〃	Ni	(SUS 316)	14	6	
2-3	SUS 316	(Ni-Cr)	0.2	8	
〃	Ni-Cr	(SUS 316)	18	5	
2-4	SUS 316	(Ni-Cr)	0.5	8	Apparent Contact Area 8.4 cm²
〃	Ni-Cr	(SUS 316)	18	12	
2-5	SUS 316	(G - 2)	0.2	2	
〃	G - 2	(SUS 316)	14	6	
2-6	G - 2	(Mo)	14	12	
〃	Mo	(G - 2)	15	14	
2-7	SUS 316	(Mo)	0.2	4	
〃	Mo	(SUS 316)	15	7	
2-8	SUS 316	(Mo)	0.2	0.8	
〃	Mo	(SUS 316)	4	5	
2-9	SUS 316	(W)	0.2	8.5	
〃	W	(SUS 316)	15	10	
2-10	SUS 316	(W)	0.2	3	Apparent Contact Area 8.4 cm²
〃	W	(SUS 316)	15	14	
2-12	SUS 316	(SUS 316)	0.2	0.5	Apparent Contact Area 8.4 cm²
〃	SUS 316	(SUS 316)	0.2	0.8	
2-13	LC-IC	(LC-IC)	0.8	1.2	
〃	LC-IC	(LC-IC)	0.8	1.0	
2-14	LW5	(SUS 316)	0.8	14	
〃	SUS 316	(LW5)	0.2	40	
2-15	SUS 316	(stellite No6)	0.2	1.5	
〃	stellite No6	(SUS 316)	0.2	0.6	
2-16	SUS 316	(SUS 316)	0.2	0.8	
〃	SUS 316	(SUS 316)	0.2	0.5	

to 0.8μ, self-welding of SUS 316 - SUS 316 combination is because the strength of material itself (because the adhesion strength of the cooling material is weaker than that of SUS 316 itself) affects the roughness change on the surface.

Those material combinations having unfilled remark column have a contact area of 220 mm^2 each. The above description represents the summary of the test results except their metallographical representation. Considerations relating to material cohesion are given as follows:

3-1. Self-Weldability of Carbide Materials.

A series of the previous tests involving Cr_3C_2 + 15 % Ni-Cr coating by plasma flame revealed, a formation of a nickel-rich diffusion layer in the cohesion boundary region indicating a trend of cohesion. This time, however, a test of chrome carbide (Cr_3C_2 + 15 % Ni-Cr) coating by D-Gun has been performed, as this material is reported as a promising padding material in the United States. Likewise, tests have been carried out with such other materials by use of W-E process as G-2 (94% WC + 6% Co) and a mixture of chrome carbide and tungsten carbide.

As indicated by Tables 4 and 6, the materials of $Cr_3 \cdot C_2$ + 15 % Ni – Cr coated by D-Gun do not cohere with their partner of the same materials. Even with SUS 316 as its partner which is easy to cohere, D-Gun did not result self-welding as did in the case of the plasma coating (Refer to Table 8). Even with the same material as chrome carbide combined, its cohesion condition is observed to be largely depended on coating methods as well as on the surface condition variation. A recent report[3] from the United States also recognizes some undesirable effect by plasma coating. Coating of this kind of material conventionally utilized plasma or oxy·acetylene, which has been a cause for unsatisfactory results and poor acceptance[4]. Since sprayed layer by D-Gun is found from our friction test to have an extremely low static

friction coefficient comparing with other materials, this material may be applicable to the real fast breeder reactor depending upon the results of further tests, for instance, irradiation test, thermal cycle test, long-term test in high purity sodium, etc.

G-2 has hitherto been widely employed for super-hard tools generally in a form of a sintered solid body. But in this form, because of poor machinability utilization of this material for FBR core structure is limited. W-E process, however, has a prospect of extending its application to ductile stainless steel surface. This experiment has had five couples on SUS 316 as the partner material under various conditions, and in four couples among five, no cohesion has been observed at all. Only one couple has been noticed a cohesion of K = 0.03 (refer to Table 5), which, however, is thought to be the result of the presence of sodium impregnated in the interface. The self-weld resistance of this material is recognized as satisfactory. LW-5 material sprayed by D-Gun, when SUS 316 is its partner material, displayed K = 0.45 cohesion strength. The porosity of the coating layer differs according to each manufacturing method of the material, and the oxygen content in the coating layer likewise changes, and thus the film condition of the contacting surface also changes. These carbide materials, if 100% is of the same material, are quite brittle and is difficult to be molded. Because of this, materials of high wettability under high temperature such as Ni, Ni-Cr, Co, etc., are mixed to the carbide. Selection of these mixing materials should carefully be made because it has influence upon self-welding. On the same couple of LC-1C material, there has been little change noticed in the surface roughness after test of these carbide materials. With

LW-5 coated stainless steel, its surface roughness changes from its original surface of 0.8μ to as much as 14μ, and at one part, the entire portion has peeled off from inside the coating layer of LW-5 material. The surface roughness of the partner material, SUS 316, changed from 0.2μ to 40μ due to transfer of LW5.

With the combination of G-2 and SUS 316, the surface roughness of G-2 which had been as large as 14μ before the test as sprayed had decreased to 6μ after the test, while the partner material SUS 316 indicated an increase of roughness from 0.2μ to 2μ. (This change, however, is still smaller comparing with the roughness of SUS 316 combined with other kind of partner material. For instance, the surface roughness of SUS 316 coupled with Ni-Cr material is 8μ, and with Ni, it is 14μ.) This is assumed as the result of the protruded particles of G-2 have mechanically intruded into SUS 316 and transited in the process of the test. Photo-1 represents the cross (sectional micrographs) of the cohesion boundary region of the self-welded LW-5 vs. SUS 316 couple. LW-5 layer shows a partial crack and numerous porosity are observed. No formation of diffusion zone is seen in the cohesion boundary region. Photo-2 shows the cross sectional micrographs of self-welded LC-1C and SUS 316 couple. (One of the two of this combination has had no cohesion.) No more than a partial micro crack is seen, which indicates a possibility to employ this combination up to this pressure. Further use may develop the crack larger and it may not endure under higher pressure condition. No formation of diffusion zone is observed in the boundary region, the same as in the case of LW-5. From this result and from the post-test surface condition it is thought that, with the combination

between LC-1C materials, it has sufficient cohesion proofness under the condition of this level. However, as LW-5 has a lower compressive characteristics than that of LC-1C, it can not be used. Even LC-1C, having such a soft material as SUS 316 for the partner material, is risky to be used under the condition of this level.

It is thought G-2 coated by W-E process, even if its partner material is SUS 316, may be used under this condition. In this case, its cohesion proofness may change, if its surface has been polished and buffed (present test was "as sprayed"). It is also thought that, its self-weld resistant property may change with the variations of residual stress and surface roughness according to the thickness of the sprayed coating layer. In this case, the configuration of the contacting area must also be considered. That is, as shown by Hertzian pressure, in the event there is a possibility of the contacting area being in a form of a point or a line, the coating thickness must be considered according to the location or position of the maximum shear stress. For this reason, consideration should be duly paid for spraying method and the adhesion strength of the coated material on the mother material. Photo-3 and 4 show the fracture surface of each material after tensile test. LC-1C with its partner material of LC-1C shows a glossy section where a slight cohesion trend has taken place. As the trend is so slight that there is hardly visible any marked change on the contacting surface (apparent contact area) comparing with the non-contacting area.

As to the previously reported hard chrome plating, the initiation of a crack was found on the surface after the test, while this LC-1C showed no crack at all on its surface. On the contrary,

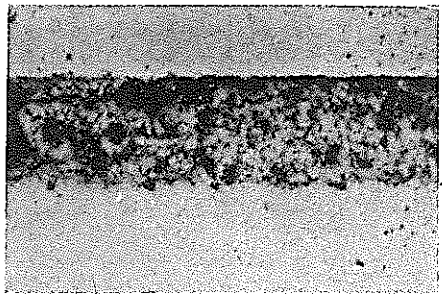

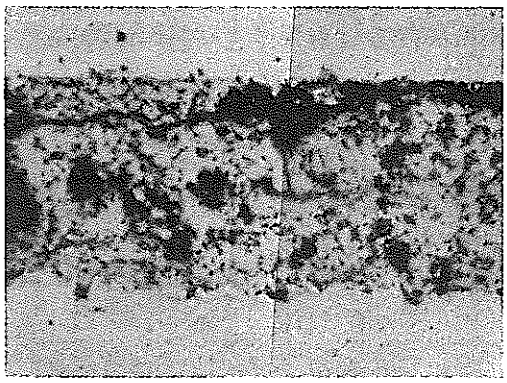

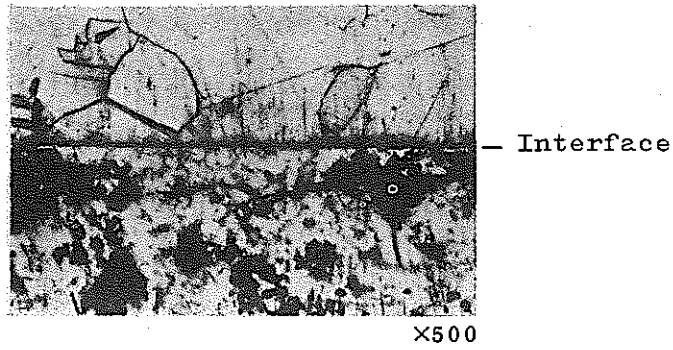

Photo. 1 Cross-Sectional Micrographs of Self-Welded SUS316 vs. LW5 Couple

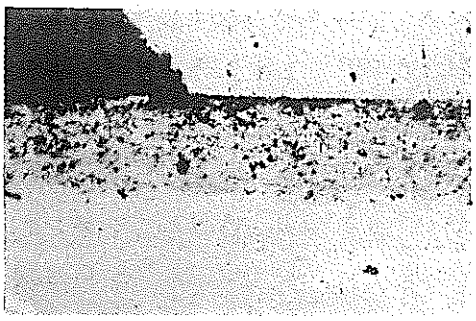

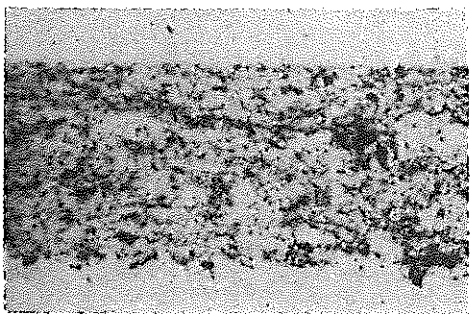

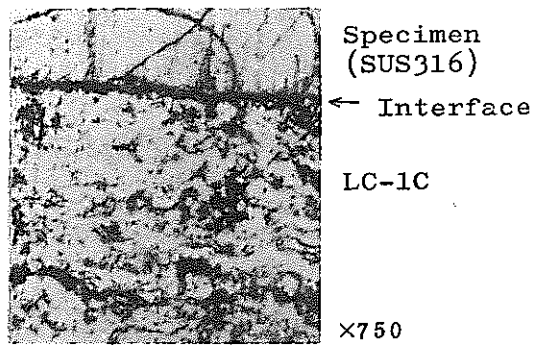

Photo. 2

Photo. 2 Cross-Sectional Micrographs of Self-Welded SUS316 vs. LC-1C Couple

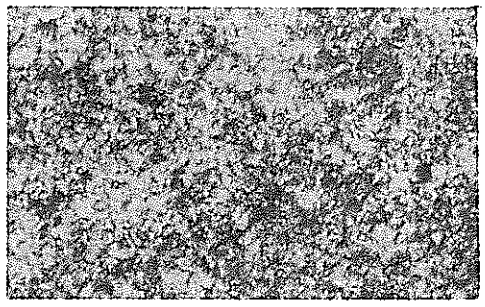

×140

Contacting Surface

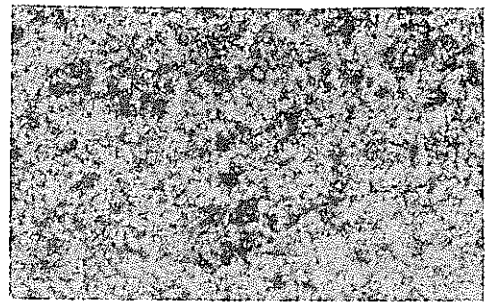

Non-Contacting Surface ×140

Photo. 3 Optical Micrographs on the Testing Surface of LCIC-LCIC Couples after Tested

Contacting Surface → | Non-Contacting Surface

×70

Testing Surface of SUS316

×280

Contacting Surface of SUS316

×70

Fracture Surface of LW-5 Side

Photo. 4 Optical Micrographs on the Fracture Surface of SUS316-LW5 Couple after Tensile Test

however, the surface of SUS 316 coupled with LW-5 showed a dark area where obviously indicated material transfer of LW-5.

The granular luster as shown in Photo-4 indicates the area where a "seizure" has taken place on the side of SUS 316 at the time of the tensile fracture after self-welding, and it is quite identical to the previously reported state of appearance observed on the fracture surface of SUS 316 after cohesion.

3-2. Self-Weldability of W and Mo Materials

In our previous report, it was reported that the plasma coated Mo material had shown a statistic factory self-weld resistant behavior. This experiment has taken up the test of Mo and W coated by W-E process. These materials have been noted for the formation of a stable oxide film in a sodium environment (easily destructable[5]). Particularly, Mo material has a large application potentiality because of its compatibility with high temperature sodium. From the previous test up to the present one, five couples with the combination of Mo and SUS 316 have undergone the tests under varied conditions. Of these five couples, only one couple showed a marked tendency to self-welding. The cohesion cross sectional micrographs of this particular test piece is shown in Photo-5. Photo-6 represents the XMA analytical results of Mo and Ni on the side of SUS 316 after fracture of the test-piece. It is evident from this photograph that Mo has transferred onto SUS 316. Photo-7 shows the surface appearance of SUS 316 when its partner material is W. The dark zone indicates the transfer of W onto SUS 316. With the combination of hard metal like W or Mo with a soft material like SUS 316, a perfect mechanical "interlocking" is seen in their surface appearance. This state of mechanical

"interlocking" offers small cohesion fracture strength while its friction coefficient has a possibility of growing higher. Four tests have been performed on the combination between W and SUS 316, and cohesion tendency has been experienced in the two couples out of these four. This cohesion strength is about 0.15 by K-value. This, however, presents a strong possibility that as the tensile test for measurement of the cohesion strength has been performed under the room temperature, the sodium present in the cohesion interface may have been solidified and produced such a level of value as K = 0.15. Generally, W and Mo coated by plasma and W-E processes have proved themselves as sufficiently self-weld resistant materials. But this does not necessarily mean that cast or forged W and Mo have also a good self weld resistant behavior. That is, as the coated W and Mo contain several per cent of Wo_2 and Mo_2 oxides[6], it can be thought that these oxides have helped to give larger self-weld resistance. Hard Cr plating is also a desirable material to form a stable film on the surface, which is referred in our previous report.

As shown in Table 6, self-weld resistance of various materials may be evaluated from the comparison of contact surface roughness, namely the change of surface roughness of the partner material (this experiment used SUS 316 which is softer than these materials) after the test. According to this evaluation, the surface roughness of SUS 316 which combined with Mo has presented less variation than in the combination with W. From this alone, it can be said that Mo is better than W as a self-weld resistant material. However, this surface roughness comparison is possible only in such combination as a slightly hard material as Mo or

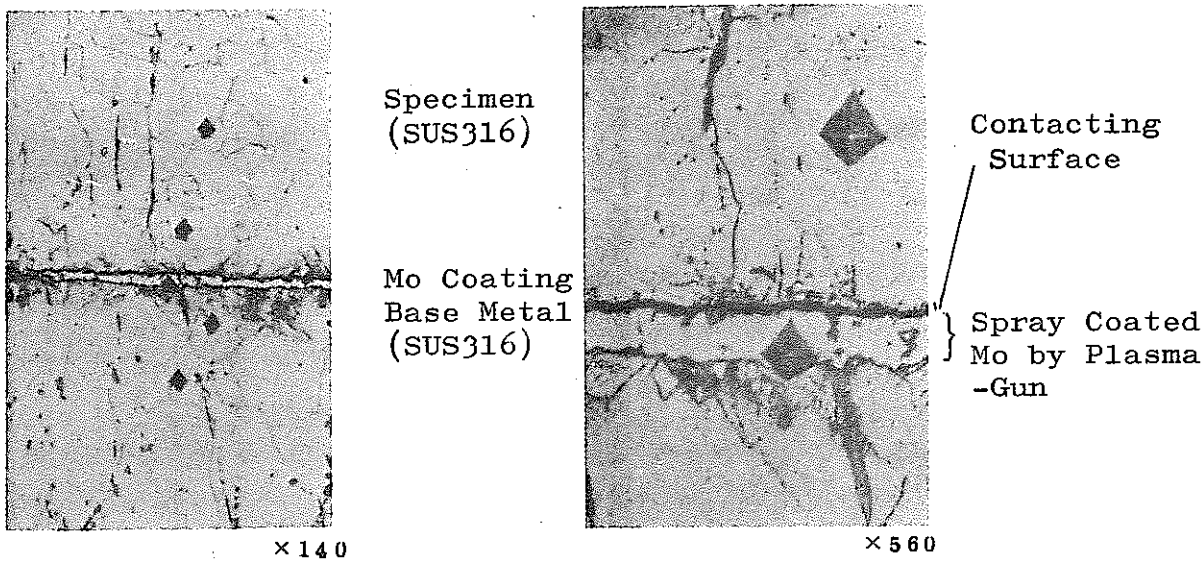

Photo. 5 Cross-Sectional Micrographs of SUS316 vs. Mo Couple

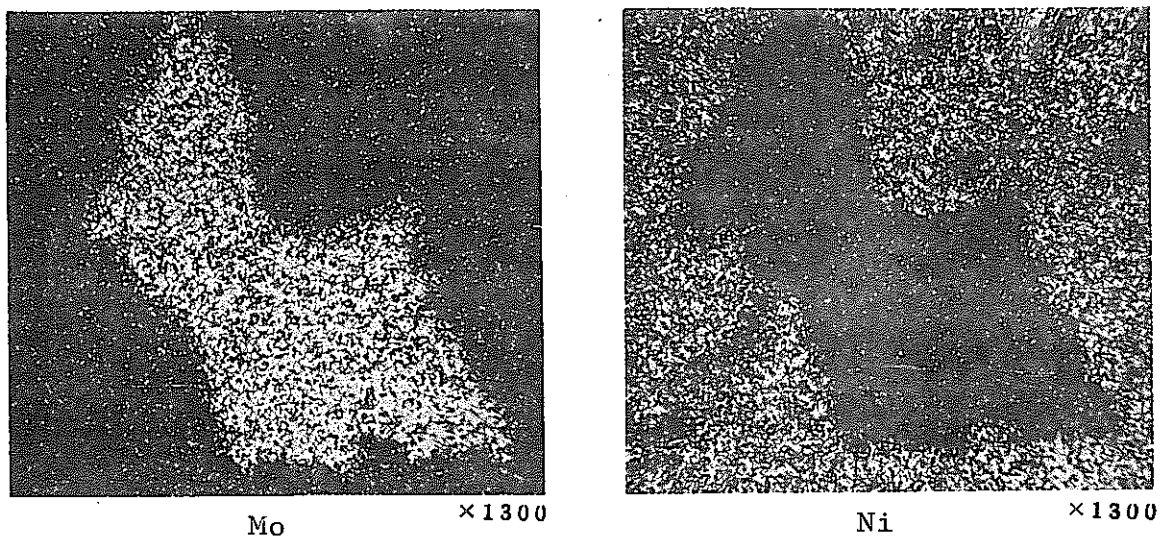

Photo. 6 Result of XMA Analysis on the Fracture Surface (SUS316) after Tension Test

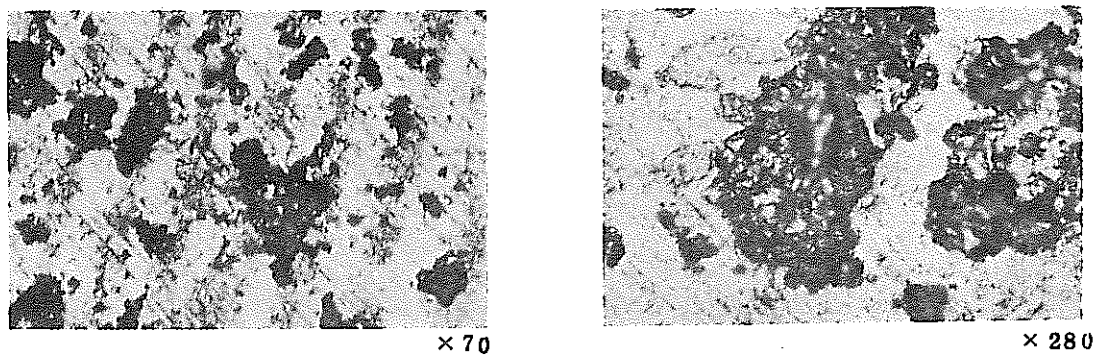

Photo. 7 Optical Micro-graphs on the Contacting Surface of SUS316 (vs. W) after Tested

W combined with a soft material as SUS 316. Other types of combination, such as SUS 316 with SUS 316 or combination between other hard materials are hardly compared. As these materials are affected by the purity of sodium, although a satisfactory result has been obtained under the present low purity sodium, as to the cohesion behavior in such a high level purity sodium as having 2 - 5 ppm oxygen concentration, it has to be further studied by performing another test (to be commenced from September, 1974.)

3-3. Self-Weldability of Ni and Ni-Cr

Ni is one of the materials to be employed for neutron absorbing body. Generally there is little chance of its being employed in FBR. But materials of this type, having a good "wettability" under high temperature, are used as a binder for sintering wear resistant materials. These binder materials can be considered to increase cohesion characteristics in sodium. Our previous report provided a description relating to formation of a preferred diffusion zone of chrome on the cohesion region of the $Cr_2 \cdot C_2$-15 % Ni·Cr material coated by plasma flame and where a self-welding has taken place. For the present test, this type of Nichrome and pure nickel were coated on SUS 316 by W-E process and its cohesion behavior was tested. Also the similar tests have been performed to seven couples of material combination such as SUS 316 with Ni, SUS 316 with Ni-Cr, Ni with Ni-Cr. The all couples of those materials were self-welded.

The cohesion strength of each of those test pieces is above 1.0 by K-value, indicating perfect self-welding. Separation occurs within the coating layer at the time of tensile fracture test. This also is endorsed by the surface roughness after fracture.

That is, the surface roughness of the partner material SUS 316 has become extremely larger than that of before the test. (Refer to Table 6).

Photo 8 shows an optical microphotograph of the cross section of the boundary region. No boundary is seen before etching, and from the after-etching structure, a diffusion layer in the boundary region is observed. From the XMA result, (Photo 9 indicates the analytical results of Ni and Cr elements in the diffusion zone. Fig. 6 shows the result of linear analysis of these zones), it is observed there are in this zone a large amount of Cr elements and a diffusion of considerable amount of Ni elements. Photo 10 and 11 represent the cross sectional structures following fracture of the test pieces of SUS 316 and Ni which cohered by the formation of the diffusion layer. (In the actual optical structure, because of the coating of Ni on the mother material SUS 316, if the partner material is SUS 316, there will exist SUS 316 on both sides.) From them, it has been learned from where fracture does initiate. The diffusion layer (which is indicated by a glossy zone in the intermediary layer in the metallographic structure) is inside the contacting surface of SUS 316, and in this region, Ni has been applied a pressure under a high temperature and made a solid diffusion on to the partner material SUS 316 during the cohesion test, and thus part of Cr has diffused from SUS 316. Particularly, in this glossy layer, the amount of Cr has tremendously increased. Besides, even with the combination between SUS 316 and Ni-Cr, this diffusion layer is quite identical. But in the combination of SUS 316 with Ni-Cr, the width of this glossy Cr rich diffusion layer is small. Photo 12

shows the optical structure of the cross section of this cohesion region.

These self-welded test pieces are tensile fractured. The tensile fracture strength is as shown by Table 5. The surface appearance of the fractured SUS 316 is shown in Photo 13. As is shown by Photo 11, the fracture has taken place in the boundary between the glossy diffusion layer and Ni, or in the Ni coating itself. XMA analytical result of this cross section is shown in Fig. 7. From this, the correlation between Na and Cr can be recognized. This can be assumed as the result of existence of $Na_xCr_YO_z$. For further investigation of its structure of diffraction, it must be relied upon a future research (for instance, such as an electron ray diffraction). Even in the case of the fractured surface of SUS 316 combined with Ni-Cr, there is observed Na - Cr correlation. Fig. 8 shows the result. Figs. 9 and 10 show respectively the XMA analytical results of the hard Cr plating surface on which formation of a film under high temperature sodium is expected, and of the surface of SUS 316 dipped into a static pot of high oxygen concentration. (Each of them presents dark colored surface after the test.) From these results, no correlation between Na and Cr has been recognized. Whether or not a film of $Na_xCr_YO_z$ exists stable in high temperature sodium and is able to produce itself is a matter of further argument. If such a film of $Na_xCr_YO_z$ is able to exist, it may act as a solid lubricant and may exercise a great influence for the subsequent friction and self-welding phenomenon.

Hanford's research has indicated that Cr containing material is good as a low friction material, and that it is because an

oxidized film of $Na_xCr_YO_z$ is formed.[7] Production of $Na_xCr_yO_z$ is affected by in-sodium oxygen concentration. Fig. 11 represents the formation energy of $Na_2Cr_2O_4$ by each oxygen concentration as quoted from the referential literature.[7,8] From this diagram, it is known that in the environment of oxygen concentration of 6 ppm level, there is little possibility of formation of $Na_2Cr_2O_4$ at temperatures above 600 °C. Under the actual operational conditions of a reactor (the oxygen concentration in "JOYO" and "MONJU" is about 10 - 20 ppm, and "FFTF" 5 ppm) no surface of component material employed in the reactor loop will allow to produce oxidized film considering from the thermal dynamic energy at 650 °C sodium temperature (or even if it is formed, it will be unstable.) Under the circumstances, as self-welding and friction phenomenon under such temperature conditions are quite unstable, it is difficult to obtain any accurate and reproducible data applicable to other items unless efforts are made to gather and accumulate more data by pursuing tests of motions and configurations more suitable and matching with the reactor components and loops.

3-4. Self-Weldability of Hard Metals and Other Materials.

It was partially reported as to the conventional Ni based colmonoy alloy in our previous report. This time, the CO based stellite No. 6 combined with SUS 316 has been subjected to a self-welding test. One of the three couples shows the cohesion fracture strength of 245 kg and 0.45 by K-value, while other two couples present no cohesion. As a result of a German test, it is reported[9] that a couple of identical materials of stellite No. 6 subjected to a test in 700 °C sodium, showed 0.59 by K-value. Photo-14 shows the surface appearance of SUS 316 at T.No.2-16

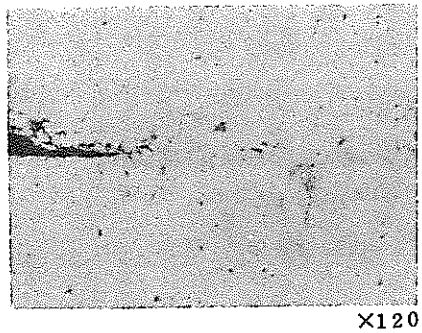

×120

before Etching

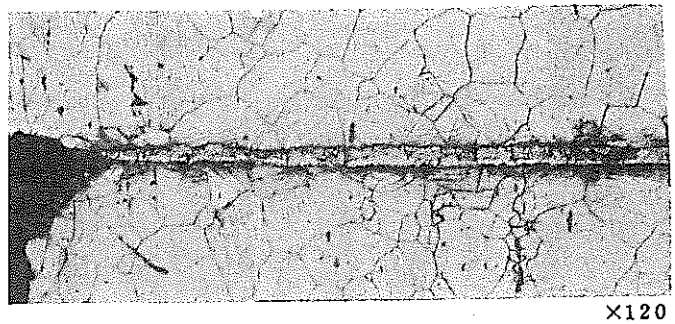

×120

after Etching

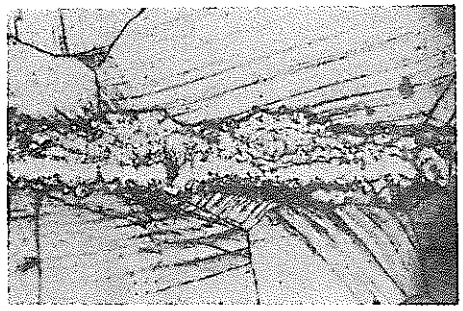

×500

Specimen (SUS316)

Contacting Surface (Testing Surface)

Ni layer

Diffusion Zone (Cr-Rich)

Base Metal (SUS316)

Photo. 8 Cross-Sectional Micrographs of Ni vs. SUS316 Couple

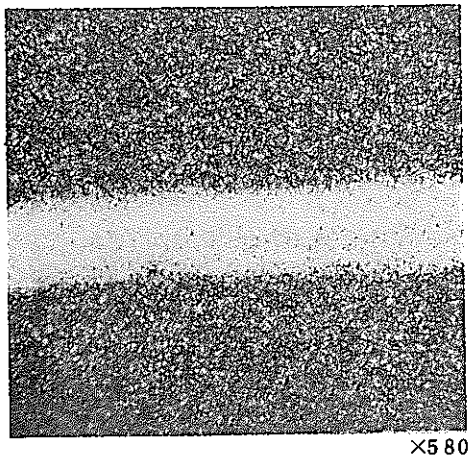

×580

Ni

Coated Ni

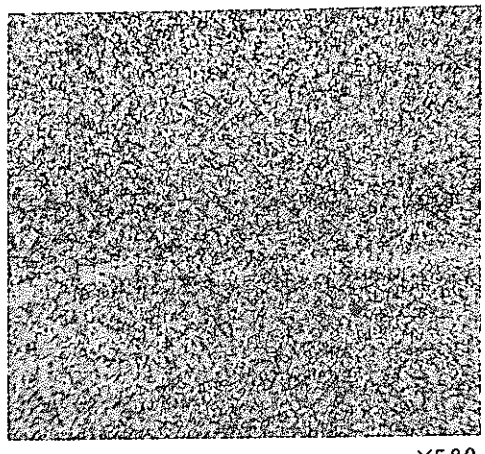

×580

Cr

Cr-Rich layer

Photo. 9 Electron Probe Microanalysis of Ni and Cr on Welded SUS316-Ni Couple

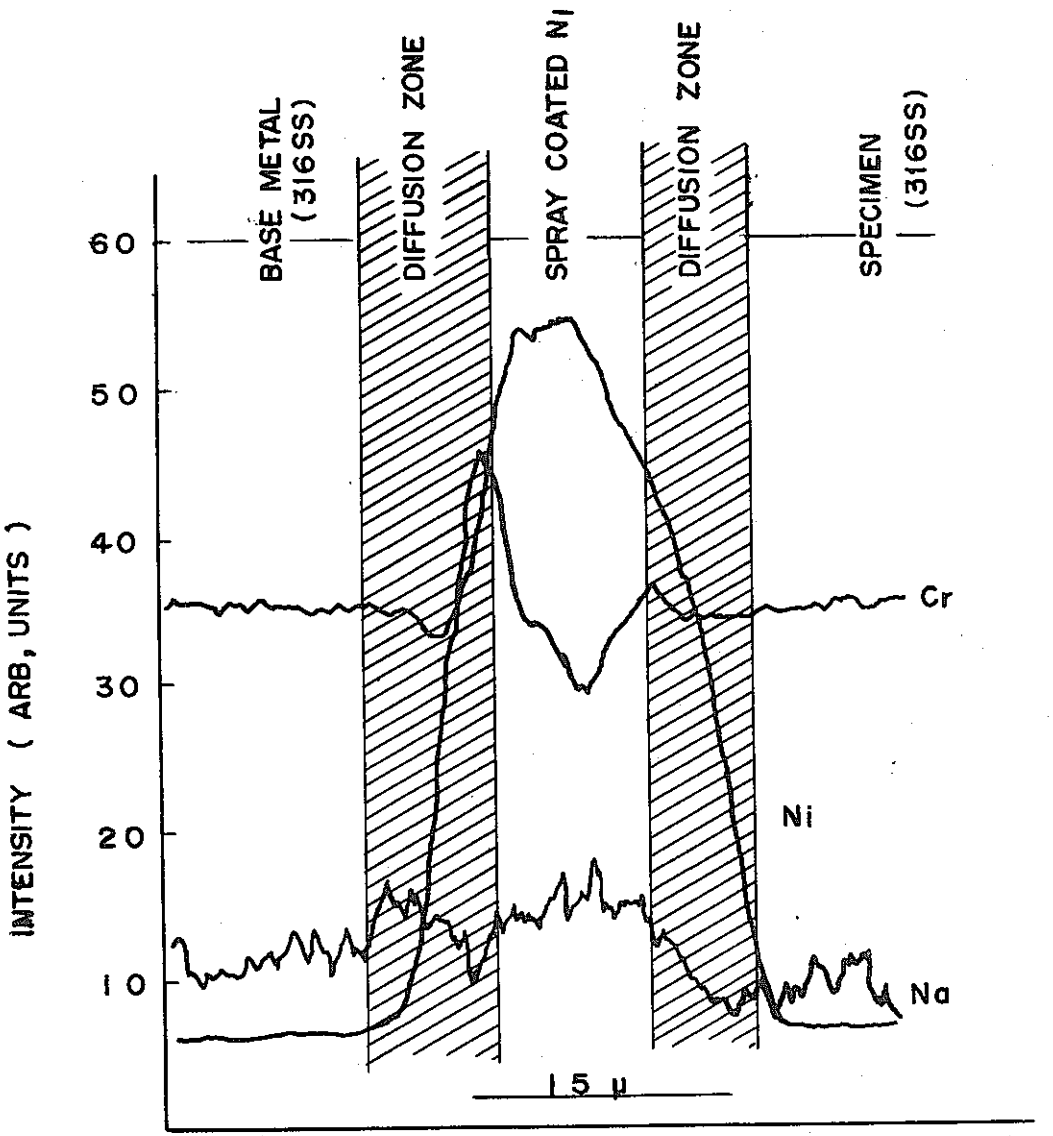

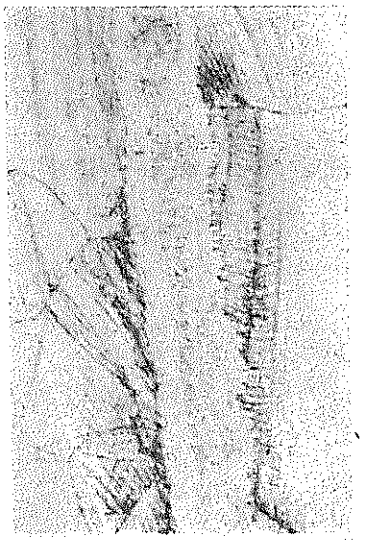

Cross-Sectional Micrograph of the Interface Area

Fig. 6 Result of XMA Analysis on Cross Section of Self Welded Specimen (316SS vs. Ni Couple)

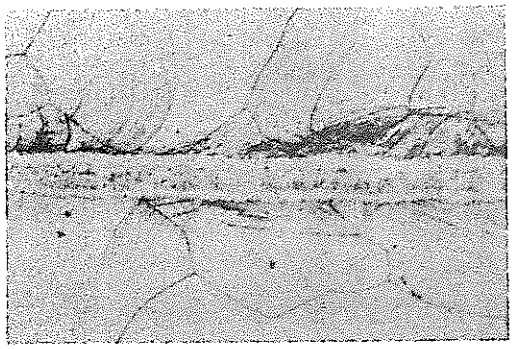

×280

×280

×560

Photo. 10 Cross-Sectional Micrographs on N_i vs. SUS316 Couple

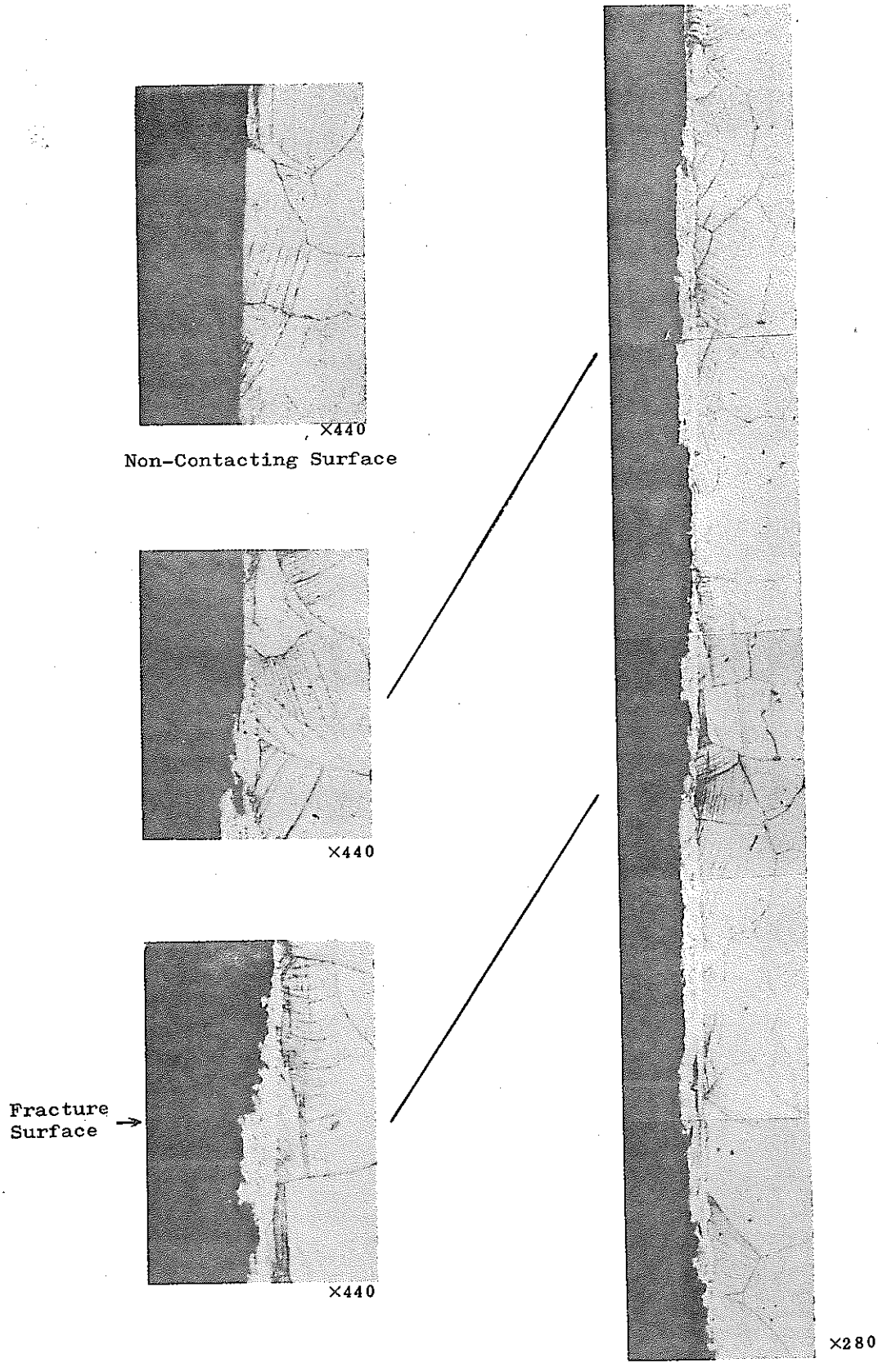

Photo.11 Cross Sectional Micrograph of 316SS Side after Tensile Test

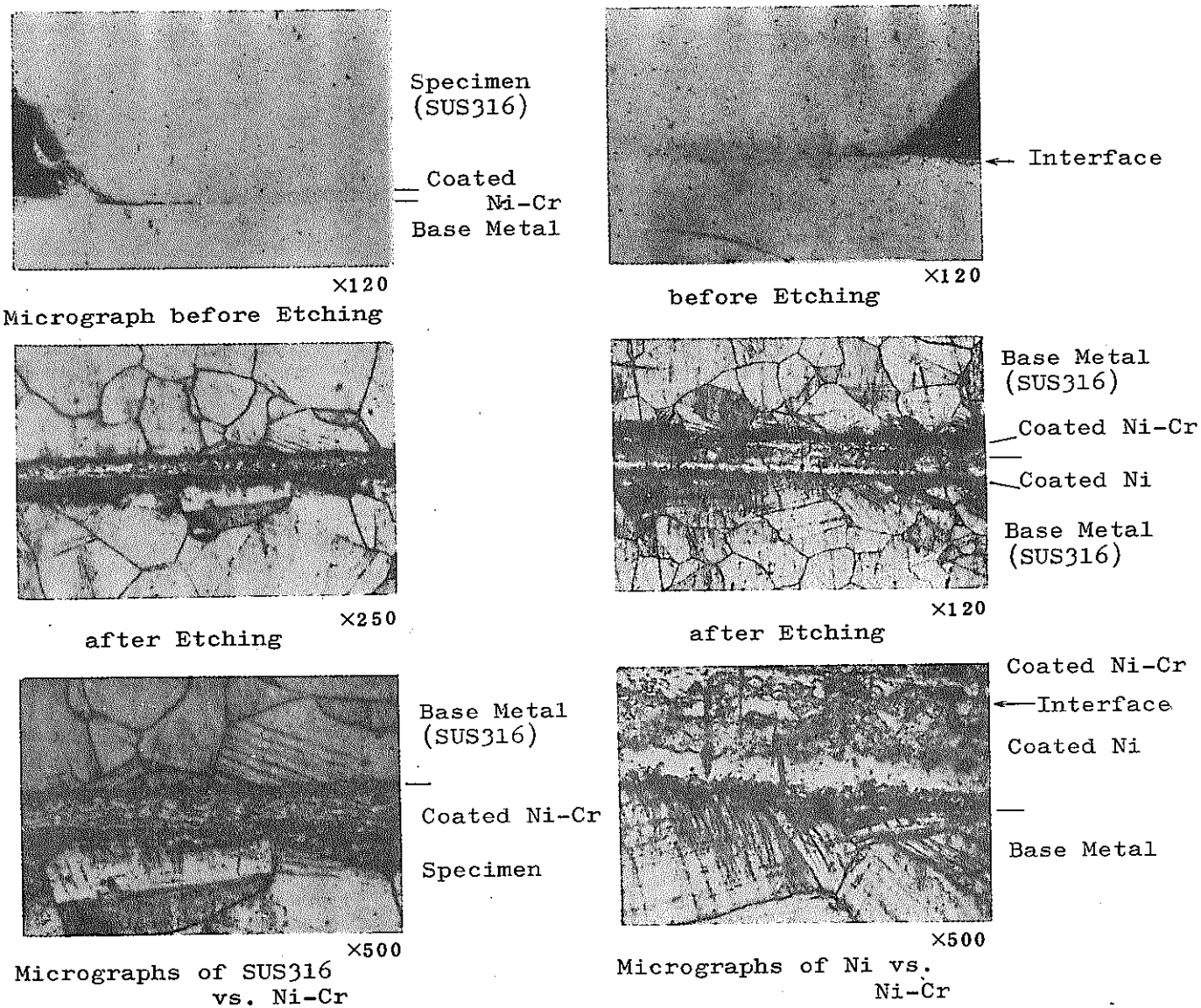

Photo.12 Cross-Sectional Micrographs of SUS316 vs. Ni-Cr and Ni vs. Ni-Cr Couples

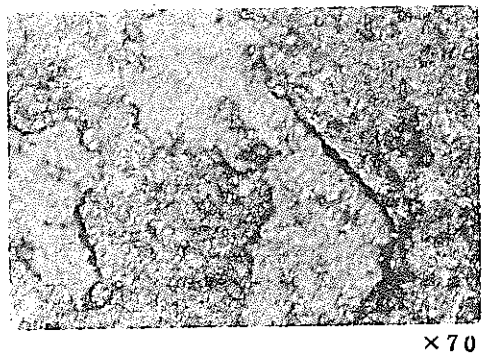

×70

Fractograph of SUS316 Side Combinated with Ni Specimen

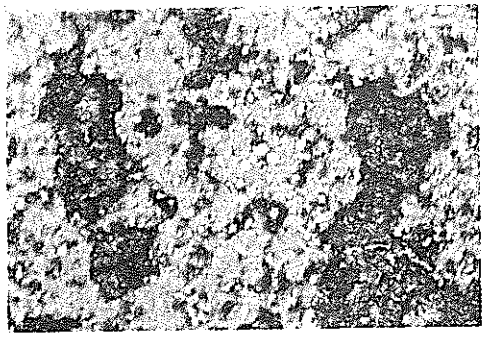

×70

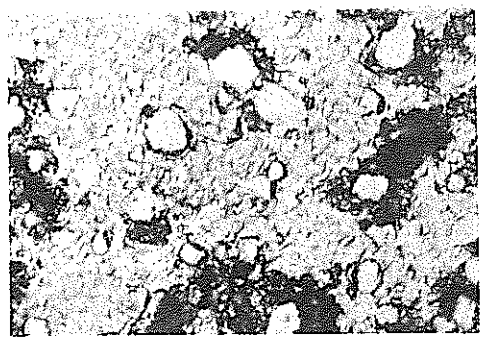

×560

Fractographs of SUS316 Side Combinated with Ni-Cr Specimen

Photo. 13 Optical Micrographs of the Fracture Surface after Tension Test

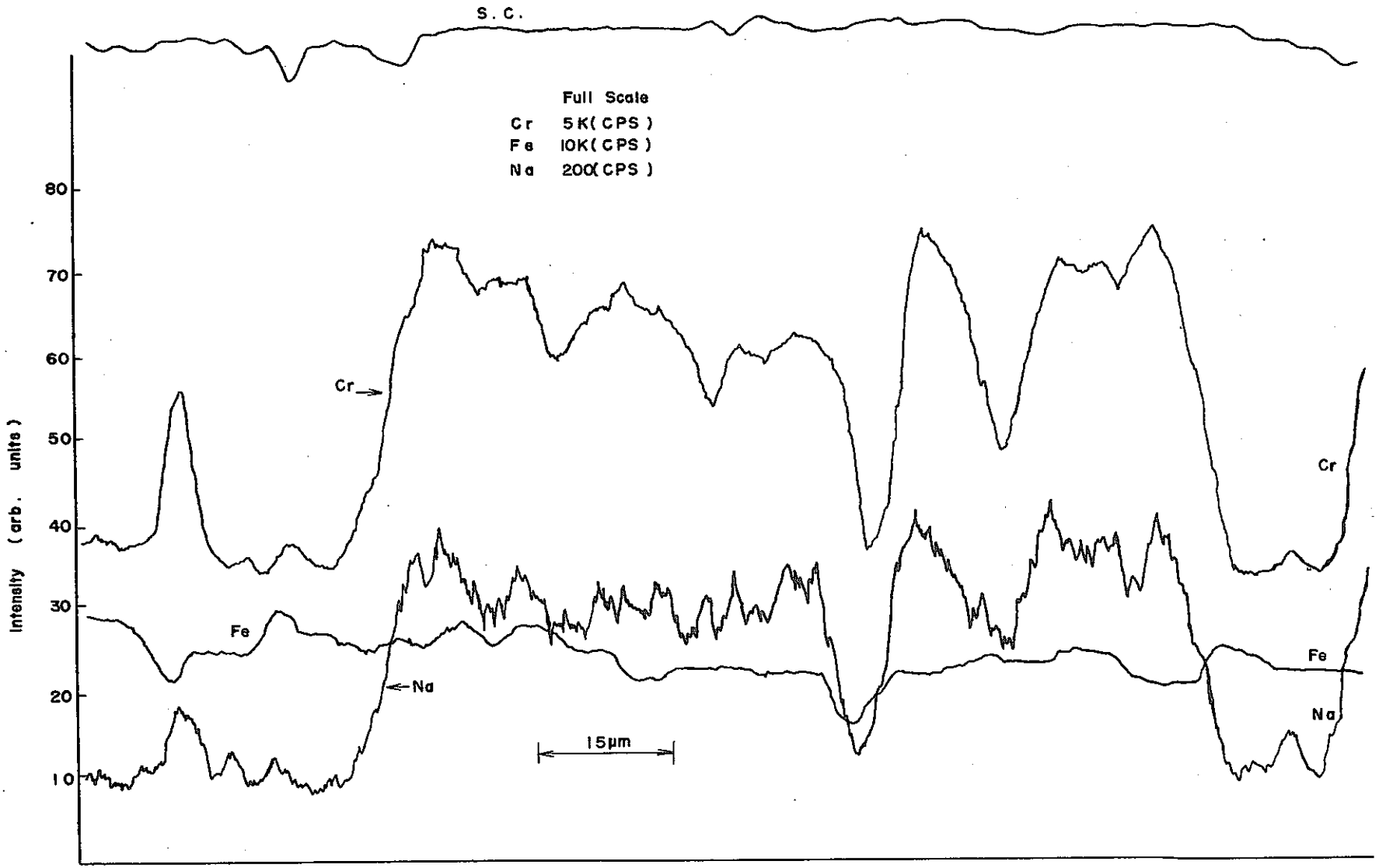

Figure 7 Result of XMA Analysis on the Fracture Surface of 316SS Side after Tensile Test

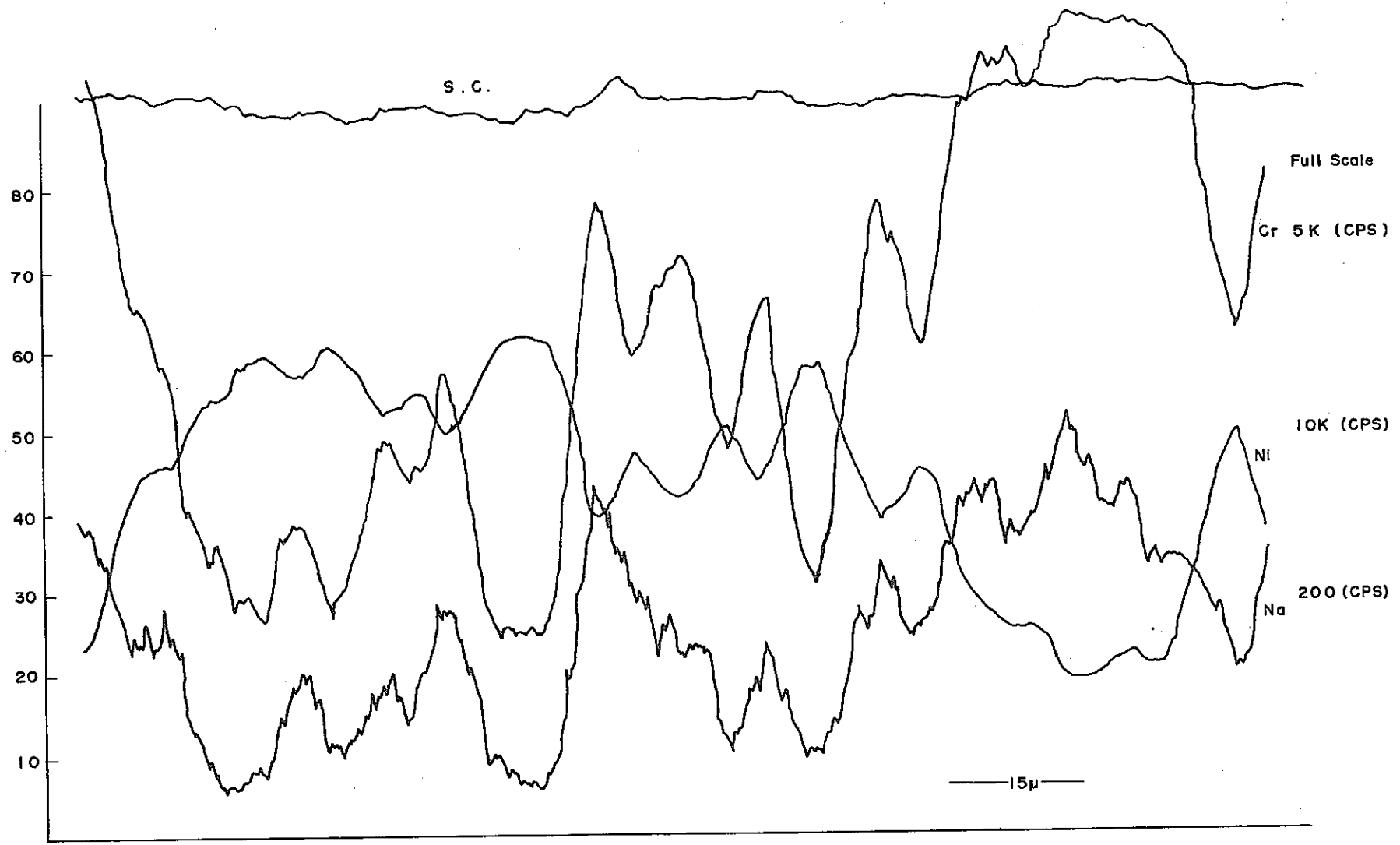

Figure 8 Result of XMA Analysis on the Fracture Surface of 316SS Side (vs. Ni-Cr) after Tensile Test

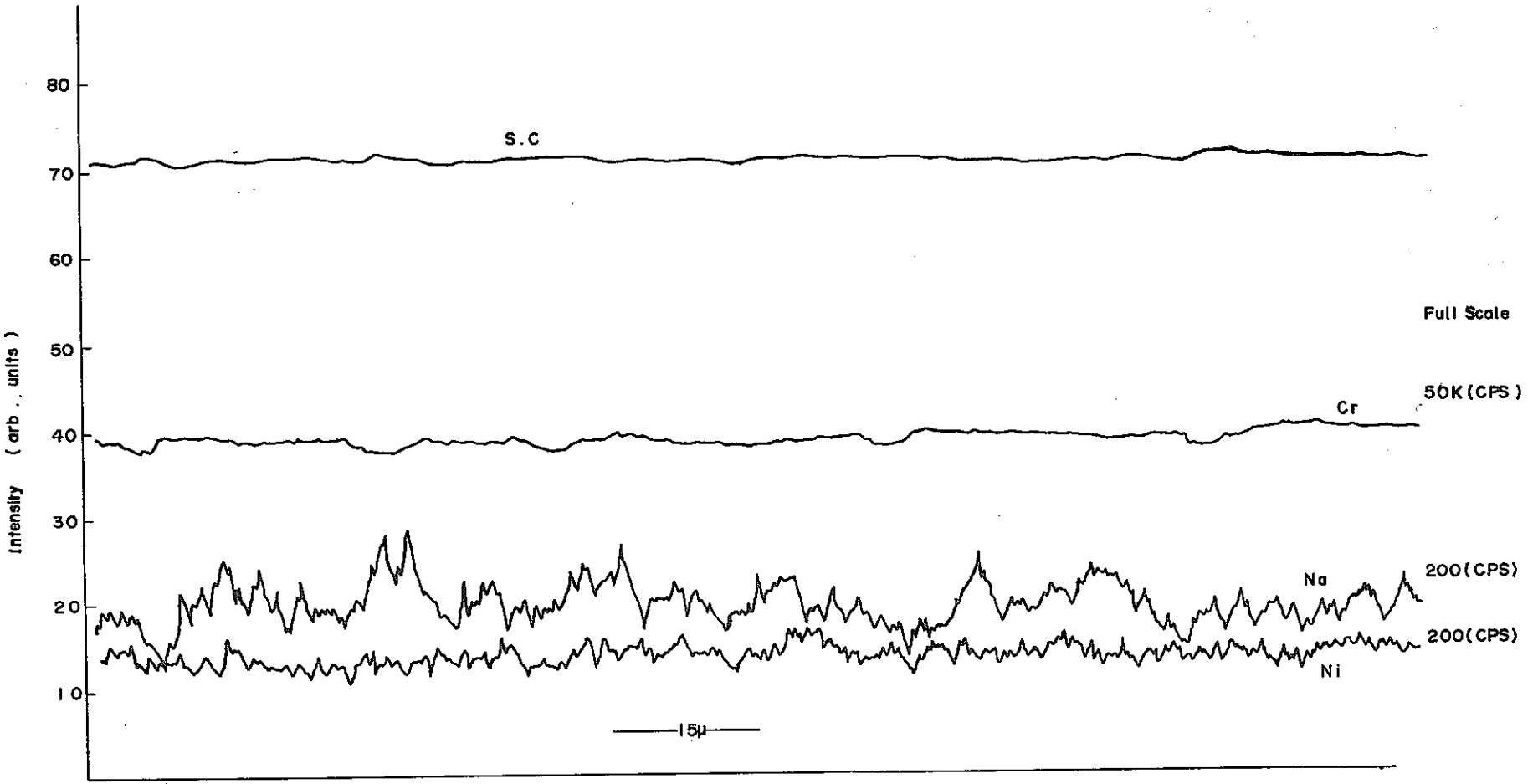

Figure 9 Result of XMA Analysis on the Surface of Hard Chrome Plating after Tested

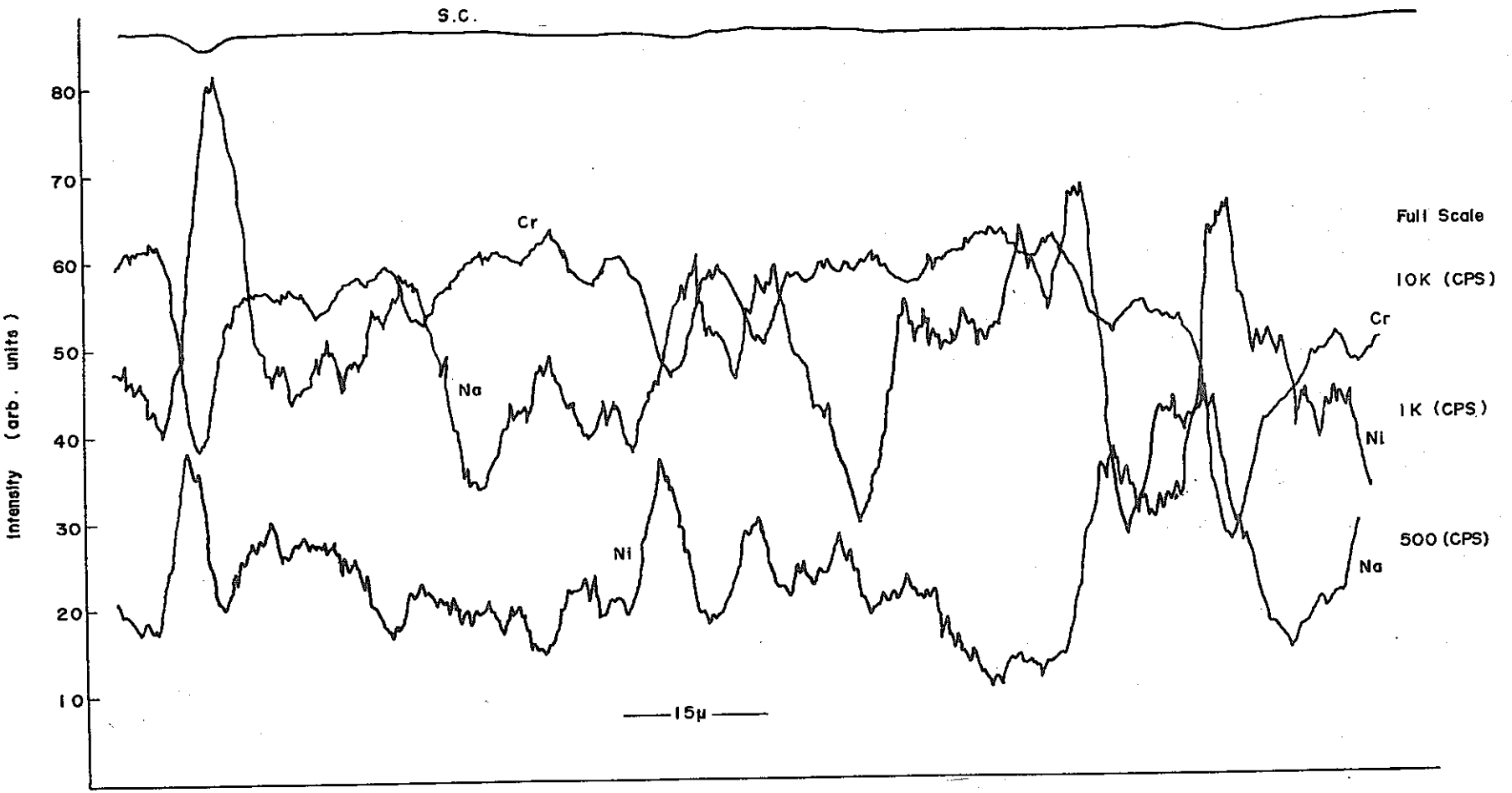

Figure 10 Result of XMA Analysis on the Surface of 316SS after Tested (under Static Na Pot Contented High Oxygen)

and that of its partner material, stellite No. 6. This evidently displays the marked difference on the surfaces between the contact area and the non-contact area. Both SUS 316 and stellite show a trend of cohesion (or deformation of true contact region) on their contact area.

At the lower part of Photo 14, the surface appearance of stellite No. 6, of which partner material SUS 316 had a fracture at T. No. 2-15 under the tensile strength of 245 kg, is shown. It indicates the similar appearance to a tensile fracture surface as shown by our previous report. That is, even stellite No. 6, if its partner material is SUS 316 shows a trend of cohesion. In our previous report, a detailed description of cohesion behavior of SUS 316 combined with its own counterpart is given, and in the present experiment, the same combination of SUS 316 under the same conditions has all presented a self-welded trend. Even such a contact area having a small contact pressure of 0.45 kg/cm^2 level has clearly indicated a cohesion trend without producing any slip line as represented by Photo 15. This suggests a possibility of cohesion of SUS 316 vs. SUS 316 without requiring too much pressure in the sodium environment at a 600 ^{o}C temperature level.

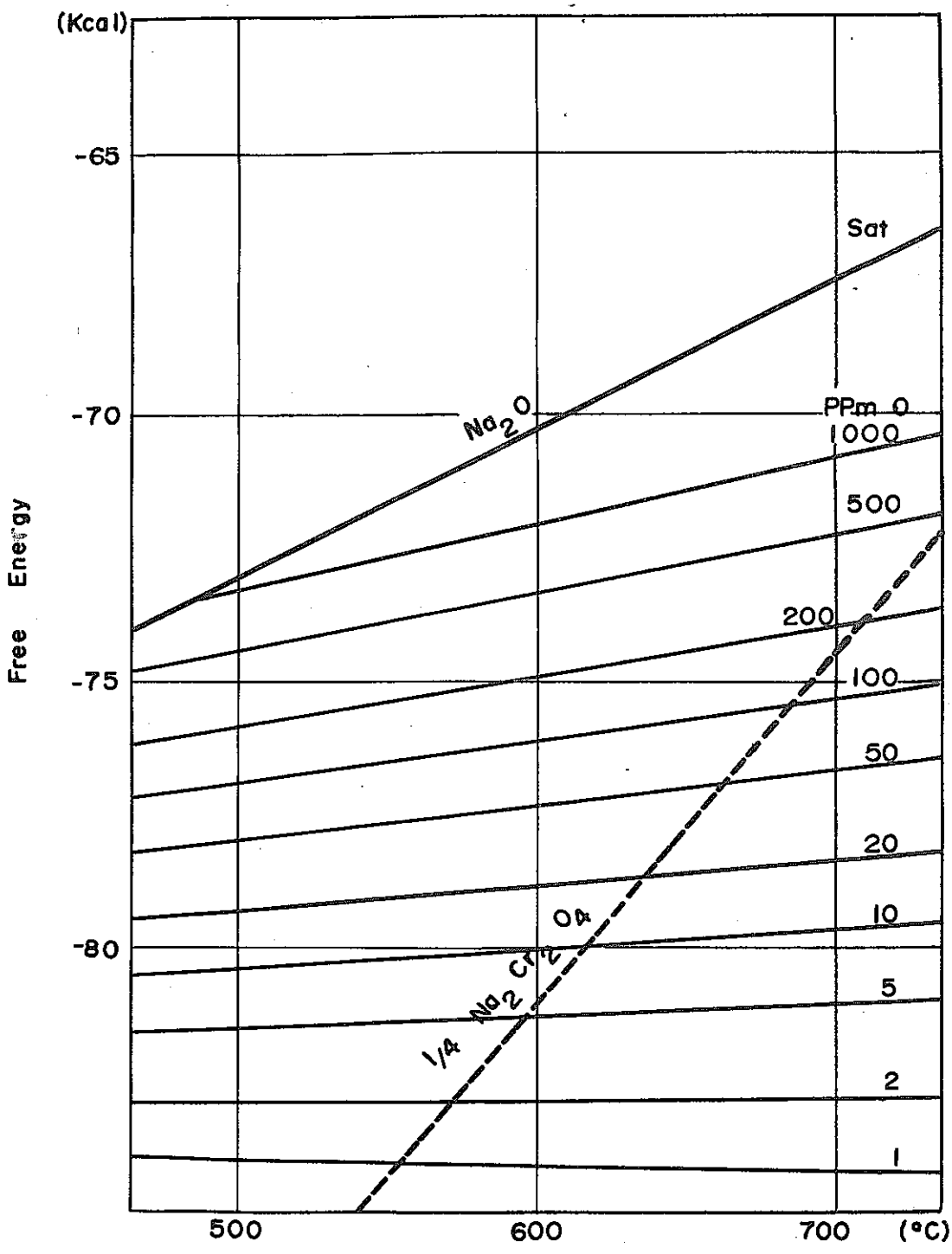

Fig.11 Free Energy of Formation of Na_2O and $Na_2Cr_2O_4$

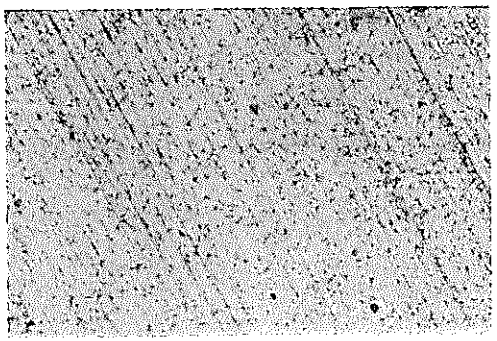

×280

Non Contacting Surface

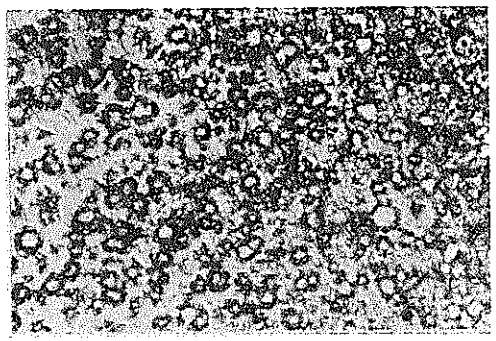

×280

Contacting Surface

316SS Side

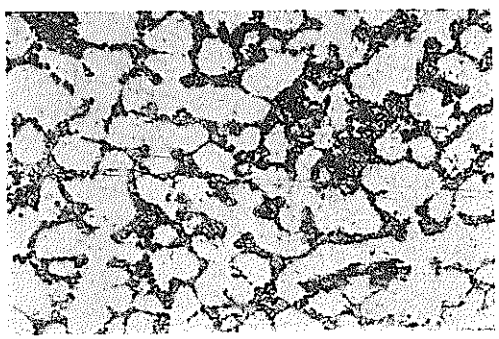

×280

Non Contacting Surface

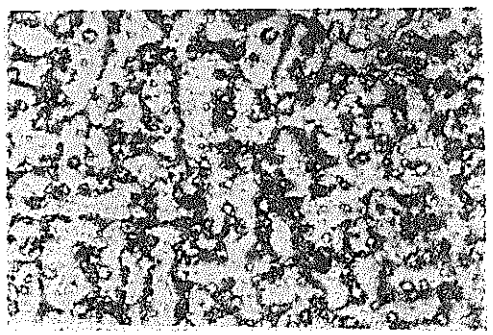

×280

Contacting Surface

Stellite
No.6 Side

Phot.14 Optical Micrographs on the Surface of 316SS-Stellite No.6 Couple after Tension Test

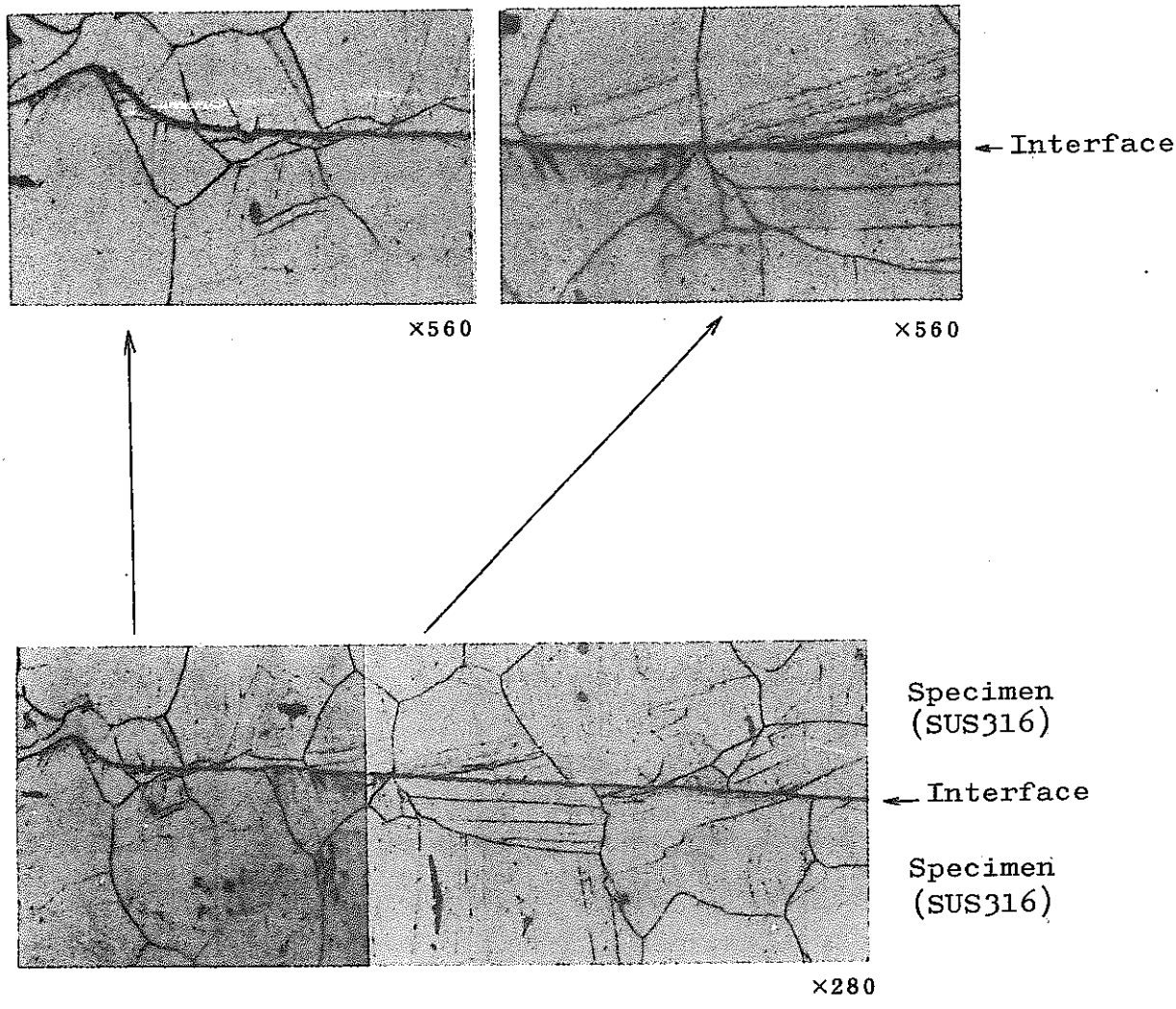

Photo. 15 Cross-Sectional Micrographs of Self-Welded SUS316 vs. SUS316 Couple after Testing at 70 kg/cm^2 in 600°C Na.

4. Conclusion

From the present experiment, the following results have been obtained.

1. Chrome carbide coated by D-Gun ($85\%Cr_3C_2 + 15\%NiCr$) is effective as self-weld resistant material.
2. Tungsten containing carbide material (25%WC + 5%Ni + 70%W-Cr carbide) has a strong tendency to self-welding, and the fracture under a tensile test has peeled off from inside of the coated layer.
3. The cohesion strength of Ni and Ni-Cr materials is extremely strong, and cohered by forming a diffusion layer. In this diffusion layer, a chrome rich zone is observed, and in the vicinity of this chrome rich zone, a correlation between Na and Cr is noticed.
4. Both materials of Mo and W are effective as self-weld resistant materials. Also, these materials as well as the W-E process coating are effective as self-weld resistant materials.
5. Stellite material has a cohesion trend when its partner material is SUS 316.

These material test results are summarized in Table 7. The values "1" showing the couple whose weldability is the highest, while "5" is the best couple for the self-weld resistant material. The determination of these weldability is made according to the results of the consideration of cohesion strength, surface roughness change after tensile fracture tests, formation of diffusion layer after all the tests (for instance, 9 couples have been performed for combination of hard Cr plating vs. hard Cr plating, none of which has had cohesion.)

The best combinations for self-weld resistant materials are hard Cr plating vs. the same, colmonoy No. 6 vs. the same, G-2 vs. SUS 316, and LC-1C vs. the same (coating applied by D-Gun).

These test results may be reflected to the design of FBR components which require no movement such as entrance nozzle, nozzle receiving plate, pads of the internal clamping, etc. For the selection of self-weld resistant materials suitable and best matching with each section of the FBR components, it may be necessary to start from the analysis of friction coefficient. (It is expected to start this work from September, 1974.)

From the series of self-welding tests so far performed, it has been found out that in the sodium of 600 ^{o}C, self-welding behavior of each material changes largely according to combination of materials and that the material selection of the contacting parts in sodium cooled fast reactor must be made carefully considering the results of these tests.

The problems of the future work relating to these material cohesion behaviors will relate to the effect upon self-welding of the oxidized film produced on the material surface and of the degradation of mechanical properties (decrease of high temperature hardness) due to the selective dissolution of alloy elements on the material surface layer, as well as of any change in alloy status (transformation to ferrite zone on the surface layer of austenitic stainless steel).

Table-7 Summary of the results of self-welding tests

Combination of materials	Weldability	Remarks
316SS vs. 316SS	1	Welded(○): 5 couples
316SS vs. 420SS	1	Welded(○): 1 couple
Hard chrome vs. Hard chrome	5	Non welding(×): 9 couples
Hard chrome vs. 316SS	4	○ : 1 × : 3
Colmonoy No. 6 vs. Colmonoy No. 6	5	× : 4
Stellite No. 6 vs. 316SS	3	○ : 1 (K=0.4) × : 2
Mo(1.2) vs. 316SS	4	○ : 1 × : 4
W(1.2) vs. 316SS	4	○ : 2 (K=0.15) × : 2
G-2(1) vs. 316SS	5	× : 4
Ni(1) vs. 316SS	1	○ : 3 (K=1.1)
Ni(1) vs. Ni-Cr	1	○ : 1
Ni-Cr(1) vs. 316SS	1	○ : 3 (K=1.1)
ICIC(2) vs. 316SS	2	○ : 2
ICIC(3) vs. 316SS	4	○ : 1 × : 1
ICIC(2) vs. ICIC(2)	3	○ : 1
ICIC(3) vs. ICIC(3)	5	× : 1
LW(3) vs. SUS 316	2	○ : 2 (K=0.45)

1 : Coatings applied by a spark-discharge deposition process from an electrode of the coating material (called wire explosion process).

2 : Plasma-Gun coating

3 : Detonation-Gun coating

5. Acknowledgement

We wish to express our deep appreciation for the cooperation of the sodium technology section, particularly to Mr. Masaaki Nemoto, who has undertaken the job of XMA analysis.

6. References

1)

2) W.A. Glaeser: Wear and Friction Characteristics of Structural Materials in Liquid Sodium Reactor Technology, Vol. 15, No. 1, Spring 1972

3) R.M. Johnson, et al.: Friction Materials for Wear Application in the FFTF USAEC Report ANL-RDP-2 (1972)

4) N.J. Hoffman, et al.: Friction and Wear Screening Tests of Materials in Sodium, LMEC-70-10 (July 15, 1970)

5) J.W. Kissel, et al.: Frictional Behavior of Sodium-Lubricated Materials in a Controlled High-Temperature Environment Wear, 5, (1962)

6)

7) J.J. Droher: Materials Compatibility in Sodium, LMEC Semiannual Technical Progress Report, LMEC 71-7, (1971)

8) B. Minushkin, et al.: Corrosion by Liquid Metals, Plenum Press, New York - London 1970, p.515

9) K. Bendorf: Experimental Investigations of Self-Welding of Structural Materials under Sodium, Nuclear Engineering and Design 14 (1970) 83 - 98